Supporting Information

Color-Tuning Pt(II) Complexes for Natural-light Electrophosphorescence

Dandan Wu,† Ke Qin,† Xin Gao,† Shuo Cheng,† Chenwei Sha,† Aoyun Wu,† Huili Ma,† Zhengyi Sun,† Cong Zhang,† and Xiao-Chun Hang*,†

†*Key Laboratory of Flexible Electronics (KLOFE) & Institute of Advanced Materials (IAM) Nanjing Tech University (NanjingTech), 30 South Puzhu Road, Nanjing 211816, China.*

AUTHOR INFORMATION

Corresponding Authors' E-mail address

Xiao-Chun Hang, E-mail: iamxchhang@njtech.edu.cn

Keywords: (Color Tuning, Broad-Spectra Emission, Electroluminescence, Phosphorescent OLEDs, Pt(II) complex, Tetradentate ligand)

General Procedures:

NMR spectra and Mass measurements. ^{1}H NMR spectra were recorded at 300 or 500 MHz on NMR instruments in chloroform-*d* or DMSO-d_6 solution, ^{13}C NMR spectra were recorded at 75 or 126 MHz on Varian Liquid-State NMR instruments in chloroform-*d* solution. Mass spectra were recorded on electrospray ionization mass spectrometry (ESI-MS).

Absorption and Emission. The UV-visible absorption spectra were recorded on a SHIMADZU UV-1750 spectrometer. Photoluminescence (PL) spectra were measured on a Hitachi F-4600 fluorescence spectrophotometer. The transient lifetimes and PLQEs were measured using on a Horiba JobinYvon Fluorolog-3 spectrometer platform. The measurement of photo-stability was carried out on the platform integrated with laser, optical fiber, spectrometer, and integrating sphere. The sample was prepared by doping the complex into polystyrene in 5 wt% concentration by spin-coating, and measured under irradiation with a beam of 500 mW/cm^2 of 375 nm laser.

Energy Level Measurements. Cyclic voltammetry was performed using a CH Instrument 660E electrochemical analyzer under a nitrogen atmosphere in glovebox. Anhydrous DMF was used as the solvent for reduction and oxidation, respectively. 0.1 M tetra(*n*-butyl) ammonium

hexafluorophosphate was used as the supporting electrolyte. A silver wire was used as the pseudo reference electrode, a Pt wire was used as the counter electrode, and platinum column was used as the working electrode. Their HOMO and LUMO energy levels were calculated from the onset of oxidation ($E_{ox,\ onset}$) and reduction potentials ($E_{red,\ onset}$) according to the equation of $E_{HOMO/LUMO} = -[E_{ox/re} - E_{(Fc/Fc+)} + 4.8]$ eV, respectively.

Thermal Properties. Thermogravimetric analysis (TGA) measurements were undertaken on NETZSCH STA 449C instrument, and the samples under nitrogen atmosphere was determined at a heating rate of 10 ^{o}C min^{-1} from 30 to 550 ^{o}C. Differential scanning calorimetry (DSC) measurements were performed on a NETZSCH DSC 200 PC unit at a heating rate of 10 ^{o}C min^{-1} from 30 to 270 ^{o}C under argon.

Computational Details. The equilibrium geometries of the ground state (S_0) were optimized by density functional theory (DFT) method using B3LYP functional together with 6-31G(d) basis set. Frequency calculations were performed to ensure structures had no imaginary frequencies. At the same level, the nature of excited singlet and triplet states, including the excitation energy and nature transition orbitals were evaluated using time-dependent density functional theory (TD-DFT). All calculations were carried out with Gaussian 09 program.

OLED Fabrication and characterization. All organic materials and electrodes were prepared on indium tin oxide (ITO) coated glass with a sheet resistance of 10 Ω/cm^2 by thermal evaporation at a base vacuum of < 1 x 10^{-7} Torr. The ITO surface was cleaned and treated by UV-ozone for 15 minutes. A shadow mask was used to define the Al cathode to form an emissive area of 9 mm^2. The evaporation rates of all organic layers were 2.0–2.2 Å/s. The evaporation rates of Liq and Al cathode were 0.2 and 4 – 6 Å/s, respectively. The doping rate was monitored with a quartz crystal monitor (QCM). Current density–luminance–voltage (J–L–V) characteristics and EL spectra of the devices were measured by Suzhou F-star Scientific Instrument. The EQE, CE and PE for PhOLEDs were measured with an integrating sphere. All devices were tested in ambient with glass lid encapsulation. Surface morphology was characterized by field-emission scanning electron microscopy (SU8010, Hitachi).

Synthesis and Structural Characterization

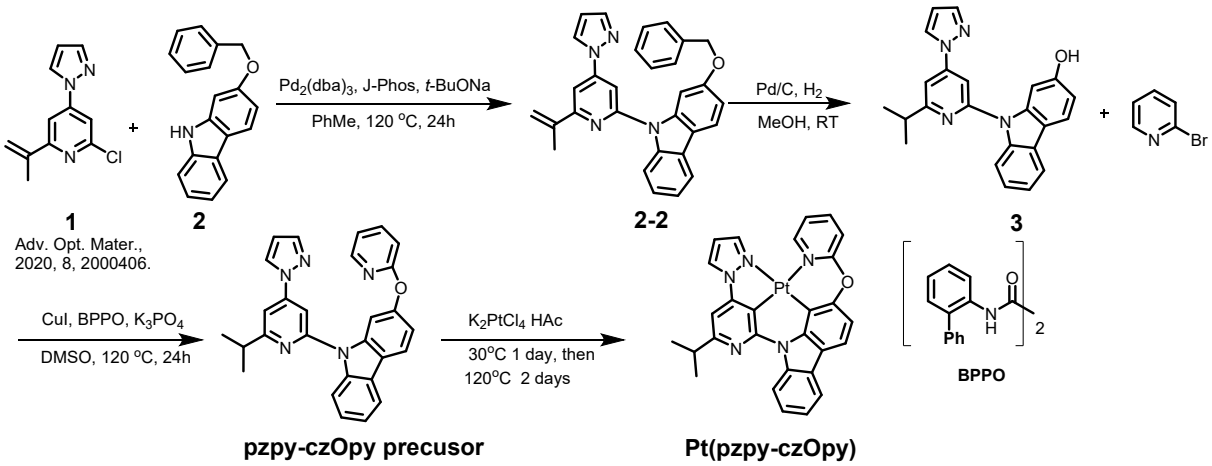

Figure S1. Synthesis of Pt(pzpy-czOpy)

Synthesis of intermediate 3

To a 15 mL sealed tube was added with 2-chloro-6-(prop-1-en-2-yl)-4-(1*H*-pyrazol-1-yl)pyridine (**1**, 219.1 mg, 1 mmol), 2-(benzyloxy)-9*H*-carbazole (273.4 mg, 1 mmol), $Pd_2(dba)_3$ (73.2 mg, 0.08 mmol), J-Phos (49.3 mg, 0.16 mmol)) ,*t*-BuONa (192.2 mg, 2 mmol) and PhMe (2 mL). The mixture was kept heating at 120 °C for 24 hours. After cooling to the room temperature, the mixture was diluted in 30 mL water, and the solution was extracted with EA (20 mL×3). The organic phases were combined, dried over anhydrous Na_2SO_4 and concentrated to give a crude product, which was further purified by column chromatography to give the product as a white solid(**2-2**, 364.7 mg, 80%).

To a 100 mL round-bottom flask was added with 2-(benzyloxy)-9-(6-(prop-1-en-2-yl)-4-(1*H*-pyrazol-1-yl)pyridin-2-yl)-9*H*-carbazole (**2-2**, 364.7 mg, 0.8 mmol), Pd/C (50 mg) and MeOH (50 mL). The mixture was bubbled with H_2 for 5 min, then kept stirring at rt for 12 hours. The reaction was monitored with TLC (PE:EA = 5:1) till completion. The mixture was added with H_2O, then extracted with EA (20 mL×3). The combined organic phase was dried with anhydrous Na_2SO_4 . The raw mixture was purified by column flash chromatography with the eluent (PE:EA = 20:1) to give a brown solid as desired product (328.2 mg, 90%). ^{1}H NMR (300 MHz, $CDCl_3$) δ 8.95 – 8.89 (d, *J* = 2.4 Hz, 1H), 8.16 – 8.12 (m, 2H), 8.11 – 8.09 (m, 2H), 7.94 – 7.90 (d, *J* = 2.0 Hz, 1H), 7.85 – 7.78 (d， *J* = 8.4 Hz, 1H), 7.60 – 7.53 (d, *J* = 2.0 Hz， 1H), 7.47 – 7.42 (m, 2H), 7.41 – 7.37 (m, 1H), 7.37 – 7.35 (m, 1H), 7.35 – 7.33 (m, 1H), 7.33 – 7.32 (m, 1H), 7.31 – 7.28 (m, 1H), 7.10 – 6.99 (m,

1H), 6.73 – 6.64 (m, 1H), 6.20 – 6.11 (s, 1H), 5.56 – 5.45 (m, 1H), 5.19 – 5.13 (s, 2H), 4.07 – 3.95 (m, 1H), 2.30 – 2.21 (s, 3H). MS (ESI) for $C_{23}H_{20}N_4O^+$ was 368.10 M^+.

Synthesis of pzpy-czOpy precursor

To a 15 mL sealed tube was added with 9-(6-isopropyl-4-(1*H*-pyrazol-1-yl)pyridin-2-yl)-9*H*-carbazol-2-ol (**3**, 276 mg, 0.75 mmol), 2-bromopyridine (237.4 mg, 1.5 mmol), CuI (28.5 mg, 0.15 mmol), BPPO (16.9 mg, 0.04 mmol)), K_3PO_4 (318 mg, 1.5 mmol) and DMSO (2 mL). The mixture was kept heating at 120 °C for 24 hours. After cooling to the room temperature, the mixture was diluted in 30 mL water, and the solution was extracted with EA (20 mL×3). The organic phases were combined, washed with water (20 mL×3), dried over anhydrous Na_2SO_4, and concentrated to give a crude product, which was further purified by column chromatography to give the product as a white solid (277 mg, 83%). ^{1}H NMR (400 MHz, DMSO-d_6) δ 8.77 (d, J = 2.8 Hz, 1H), 8.24 – 8.16 (m, 2H), 8.12 (dd, J_1 = 4.8 Hz, J_1 = 1.6 Hz, 1H), 7.99 (d, J = 1.6 Hz, 1H), 7.89 – 7.71 (m, 4H), 7.66 (d, J = 2.0 Hz, 1H), 7.47 – 7.39 (m, 1H), 7.34 – 7.26 (m, 1H), 7.16 – 6.96 (m, 3H), 6.67 – 6.54 (m, 1H), 3.07 (sept, J = 6.9 Hz, 1H), 1.20 (d, J = 6.9 Hz, 6H).^{13}C NMR (101 MHz, , DMSO-d_6) δ 169.26, 151.92, 151.82, 148.83, 146.86, 143.24, 139.97, 139.94, 139.75, 134.53, 129.47, 129.44, 127.75, 127.34, 123.86, 123.10, 122.02, 122.00, 121.58, 121.44, 121.25, 120.92, 120.72, 117.08, 116.20, 112.09, 111.20, 110.89, 109.78, 108.06, 105.00, 36.31, 22.63 (2C). MS (ESI) for $C_{28}H_{24}N_5O^+$ was 446.10 $[M+H]^+$.

Synthesis of Pt(pzpy-czOpy)

To a 48 mL sealed tube was added with 9-(6-isopropyl-4-(1*H*-pyrazol-1-yl)pyridin-2-yl)-2-(pyridin-2-yloxy)-9*H*-carbazole (37 mg, 0.08 mmol), K_2PtCl_4 (38 mg, 0.09 mmol) and HAc (10 mL). The mixture was bubbled with N_2 for 30 minutes. The reaction was stirred at 30 °C for 24 hours, and then slowly heated to 120 °C and kept stirring at 120 °C for 48 hours. The reaction was monitored with TLC (DCM:PE = 1:1) till completion. After cooling to rt, the mixture was added with H_2O and extracted with DCM (20 mL×3). The combined organic phase was washed with water (20 mL×3), dried over anhydrous Na_2SO_4, and concentrated in vacuum after removing the inorganic salts. The raw mixture was purified by flash column chromatography with the eluent (DCM:PE = 1:3) to give a yellow solid as desired product (15 mg, 30% yield). ^{1}H NMR (400 MHz, , DMSO-d_6) δ 9.64 (d, J = 8.4 Hz, 1H), 9.05 (d, J = 2.8 Hz, 1H), 8.92 (dd, J_1 = 5.6 Hz, J_2 = 1.6 Hz, 1H), 8.26 – 8.20 (m, 1H), 8.17 – 811 (m, 2H), 7.94 (d, J = 8 Hz, 1H), 7.59 (dd, J_1 = 8.4 Hz, J_2 = 0.8 Hz, 1H), 7.52 (s, 1H), 7.50 – 7.44 (m, 1H), 7.42 – 7.36 (m, 1H), 7.32 – 7.27 (m, 1H), 7.19 (d, J = 8 Hz, 1H), 6.95 – 6.89 (m, 1H), 3.18 (sept, J = 6.8 Hz, 1H), 1.45 (d, J = 6.8 Hz, 6H). ^{13}C NMR (126 MHz, $CDCl_3$) δ 161.36, 157.83, 152.99, 151.87, 151.47, 148.59, 140.88, 139.82, 138.89, 138.83,

127.05, 126.32, 124.80, 120.68, 119.15, 118.63, 118.26, 118.20, 115.90, 115.12, 110.09, 107.42, 107.02, 98.48, 98.39, 36.45, 22.98 (2C). MS (ESI) for $C_{28}H_{22}N_5OPt^+$ was 639.14 $[M+H]^+$, HR-MS for $C_{28}H_{22}N_5OPt^+$ $[M+H]^+$ is 639.1647, Found 639.1647.

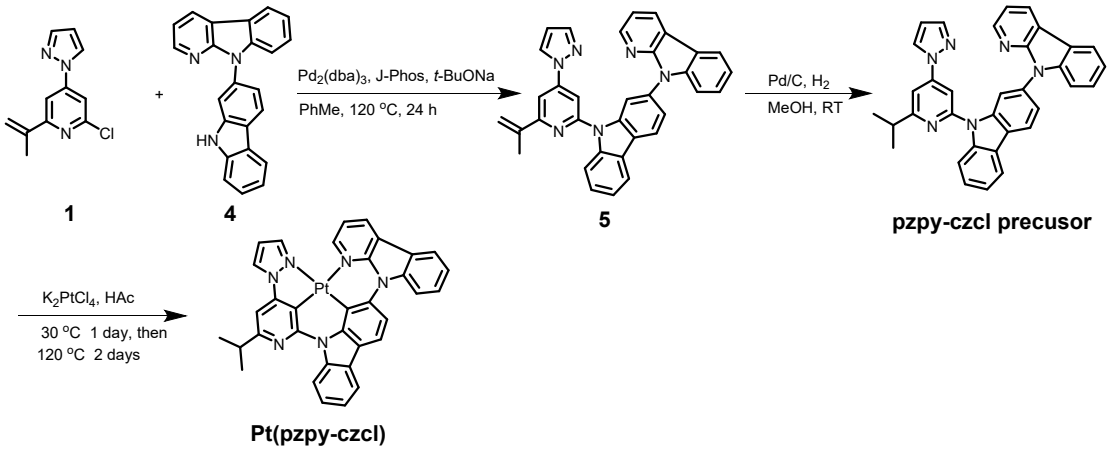

Figure S2. Synthesis of Pt(pzpy-czcl)

Synthesis of pzpy-czcl precursor

To a 15 mL sealed tube was added with 9-(9*H*-carbazol-2-yl)-9*H*-pyrido[2,3-b] indole (333.2 mg, 1 mmol), 2-chloro-6-(prop-1-en-2-yl)-4-(1*H*-pyrazol-1-yl) pyridine (438 mg, 2 mmol), $Pd_2(dba)_3$ (73.2 mg, 0.08 mmol), J-Phos (49.3 mg, 0.16 mmol)) ,*t*-BuONa (192.2 mg, 2 mmol) and PhMe (2 mL). The mixture was kept heating at 120 °C for 24 hours. After cooling to the room temperature, the mixture was diluted in 30 mL water, and the solution was extracted with EA (20 mL×3). The organic phases were combined, dried over anhydrous Na_2SO_4 and concentrated to give a crude product, which was further purified by column chromatography to give the product as a white solid (**5**, 413 mg, 80%).^{1}H NMR (400 MHz, DMSO-d_6) δ 8.87 (d, J = 2.4 Hz, 1H), 8.61 (m, 1H), 8.46 (d, J = 8 Hz, 1H), 8.40 (m, 1H), 8.34 (d, J = 8 Hz,1H), 8.26 (d, J = 7.6 Hz,1H), 8.20 (d, J = 2 Hz, 1H), 8.16 (d, J = 1.2 Hz, 1H), 8.02 (d, J = 1.2 Hz, 1H), 7.94 (d, J = 8.4 Hz, 1H), 7.86 (d, J = 1.6 Hz, 1H), 7.65 – 7.59 (m, 2H), 7.50 (m, 2H), 7.39 (t, J = 7.6 Hz, 1H), 7.35 – 7.28 (m, 2H), 6.66 – 6.61 (m, 1H), 6.13 (s, 1H), 5.39 (s, 1H), 2.15 (s, 3H). MS (ESI) for $C_{34}H_{27}N_6$ was 517.21 $[M+H]^+$

To a 100 mL round-bottom flask was added with 9-(9-(6-(prop-1-en-2-yl)-4-(1*H*-pyrazol-1-yl)pyridin-2-yl)-9*H*-carbazol-2-yl)-9*H*-pyrido[2,3-b]indole (**5**, 40 mg, 0.09 mmol), Pd/C (5 mg) and MeOH (5mL). The mixture was bubbled with H_2 for 5 min, then kept stirring at rt for 12 hours. The

reaction was monitored with TLC (PE:EA = 5:1) till completion. The mixture was added with H_2O, then extracted with EA (20 mL×3). The combined organic phase was dried with anhydrous Na_2SO_4 . The raw mixture was purified by column flash chromatography with the eluent (PE:EA = 20:1) to give a white solid as desired product (37 mg, 93%). ^{1}H NMR (400 MHz, DMSO-d_6) δ 8.80 (d, J = 2.4 Hz, 1H), 8.63 (dd, J_1 = 7.6 Hz, J = 2.0 Hz, 1H), 8.48 (d, J = 8.4 Hz, 1H), 8.41 (dd, J_1 = 4.8 Hz, J = 1.6 Hz, 1H), 8.37 – 8.33 (m, 1H), 8.30 – 8.27 (m, 1H), 8.25 (d, J = 1.6 Hz, 1H), 8.11 (d, J = 1.6 Hz, 1H), 7.95 (d, J = 8.4 Hz, 1H), 7.86 (d, J = 1.6 Hz, 1H), 7.78 (d, J = 2 Hz, 1H), 7.69 – 7.62 (m, 2H), 7.58 – 7.47 (m, 2H), 7.44 – 7.38 (m, 1H), 7.37 – 7.30 (m, 2H), 6.64 (dd, J_1 = 2.8 Hz, J = 2.0 Hz, 1H), 3.12 (sept, J = 6.8 Hz, 1H), 1.24 (d, J = 6.8 Hz, 6H).^{13}CNMR (126 MHz, $CDCl_3$) δ 152.30, 151.76, 149.56, 149.20, 149.17, 145.47, 144.24, 141.27, 140.53, 140.06, 139.54, 136.08, 130.70, 130.52, 128.10, 127.35, 126.28, 124.87, 124.36, 123.45, 120.60, 119.19, 119.03, 118.57, 115.64, 114.70, 114.39, 113.90, 108.73, 107.40, 98.27, 36.63, 23.01(2C). MS (ESI) for $C_{34}H_{27}N_6$ was 519.31 $[M+H]^+$.

Synthesis of Pt(pzpy-czcl)

To a 48 mL sealed tube was added with 9-(6-isopropyl-4-(1*H*-pyrrol-1-yl)pyridin-2-yl)-*N*-phenyl-*N*-(pyridin-2-yl)-9*H*-carbazol-2-amine (41.6 mg, 0.08 mmol), K_2PtCl_4 (38 mg, 0.09 mmol) and HAc (10 mL). The mixture was bubbled with N_2 for 30 minutes. The reaction was stirred at 30 °C for 24 hours, and slowly heated to 120 °C and kept stirring at 120 °C for 48 hours. The reaction was monitored with TLC (DCM:PE = 1:1) till completion. After cooling to rt, the mixture was added with H_2O and extracted with DCM (20 mL×3). The combined organic phase was washed with water (20 mL×3), dried over anhydrous Na_2SO_4, and concentrated in vacuum. The raw mixture was purified by column flash chromatography with the eluent (DCM:PE = 1:3) to give a yellow solid as desired product (17 mg, 30% yield). ^{1}H NMR (400 MHz, DMSO-d_6) δ 9.65 (d, J = 8.4 Hz, 1H), 9.19 (d, J = 5.6 Hz, 1H), 9.09 – 9.04 (m, 2H), 8.45 (d, J = 7.6 Hz, 1H), 8.26 (d, J = 8.4 Hz, 1H), 8.21 (d, J = 7.6 Hz, 1H), 8.09 (d, J = 2.4 Hz, 1H), 8.05 (d, J = 8.0 Hz, 1H), 7.84 (d, J = 8.4 Hz, 1H), 7.71 – 7.64 (m, 2H), 7.56 – 7.48 (m, 3H), 7.36 – 7.30 (m, 1H), 6.93 – 6.90 (m, 1H), 3.34 (sept, J = 6.8 Hz, 1H), 1.47 (d, J = 6.8 Hz, 6H). ^{13}C NMR (126 MHz, $CDCl_3$) δ 161.27, 152.66, 151.43, 145.56, 145.41, 142.13, 139.91, 139.82, 139.54, 134.56, 127.60, 127.33, 126.67, 126.22, 125.12, 121.76, 121.71, 120.95, 120.62, 119.60, 119.11, 118.78, 118.69, 115.76, 115.03, 114.13, 111.79, 108.82, 107.36, 106.94, 98.31, 36.45, 23.01(2C). MS (ESI) for $C_{34}H_{25}N_6OPt^+$ was 712.12 $[M+H]^+$, HR-MS for $C_{34}H_{25}N_6OPt^+$ $[M+H]^+$ is 712.1783, Found 712.1777.

Electrochemistry

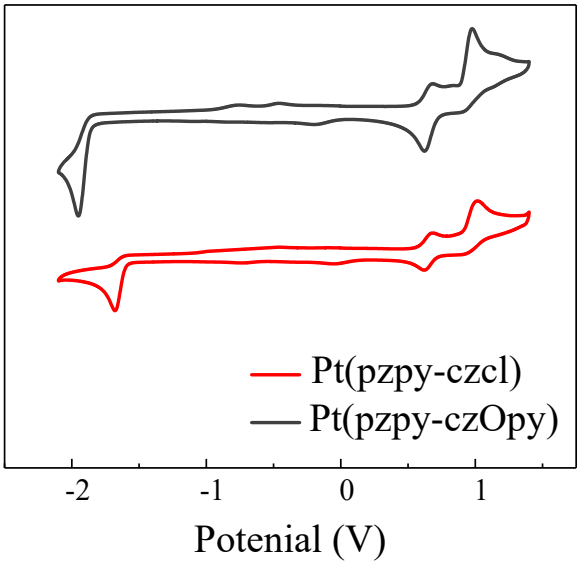

Figure S3 Cyclic voltammetry tests.

Thermal Properties

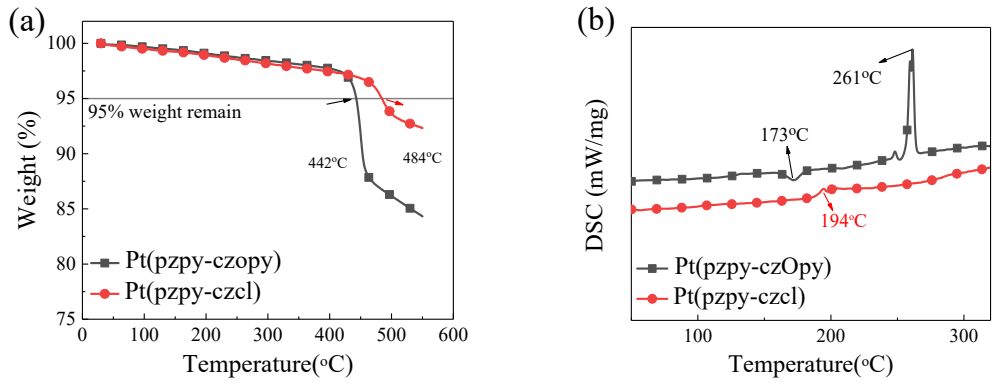

Figure S4 Thermal gravimetric analysis (TGA) and different scanning calorimetry (DSC) analysis.

Photophysical Properties

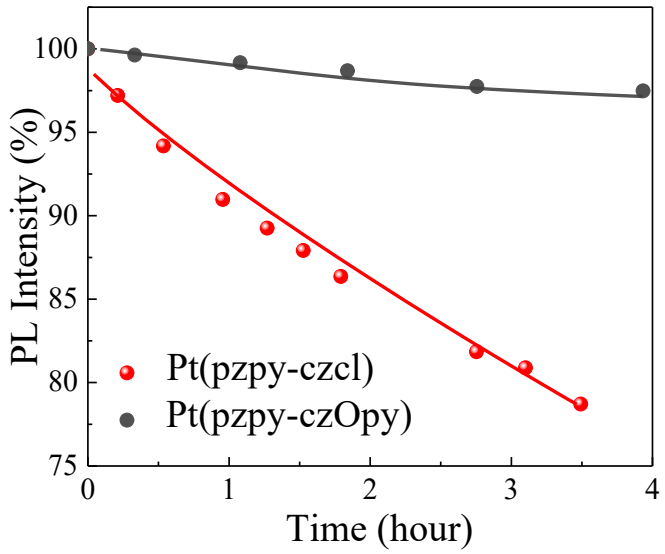

Figure S5. Photo-degradation analysis.

Table S1. Concentration-depended photoluminescent data [a]

Doping [%]	λ [nm]	FWHM [nm]	Φ [%]	τ [b] [μs]	k_r [10^5 s^{-1}]	k_{nr} [$10^5 s^{-1}$]
1 %	462 / 477	58 / 67	56 / 7	5.0 / 3.6	1.1 / 0.2	0.8 / 2.6
5 %	465 / 500	73 / 96	72 / 44	4.4 / 2.6	1.6 / 1.7	0.6 / 2.2
10 %	493 / 511	101 / 98	56 / 34	3.4 / 2.4	1.6 / 1.4	1.2 / 2.8
20 %	521 / 513	115 / 106	51 / 25	2.3 / 2.7	2.2 / 0.9	2.1 / 2.8
50 %	523 / 530	117 / 118	15 / 21	2.2 / 2.1	0.6 / 1.0	3.8 / 3.8
75 %	531 / 553	121 / 105	11 / 14	1.3 / 1.2	0.8 / 1.2	6.4 / 7.4

[a] The front and back values of "– / –" are the data of Pt(pzpy-czOpy) and Pt(pzpy-czcl), respectively. [b] The average radiative decay lifetimes.

Computational Simulations

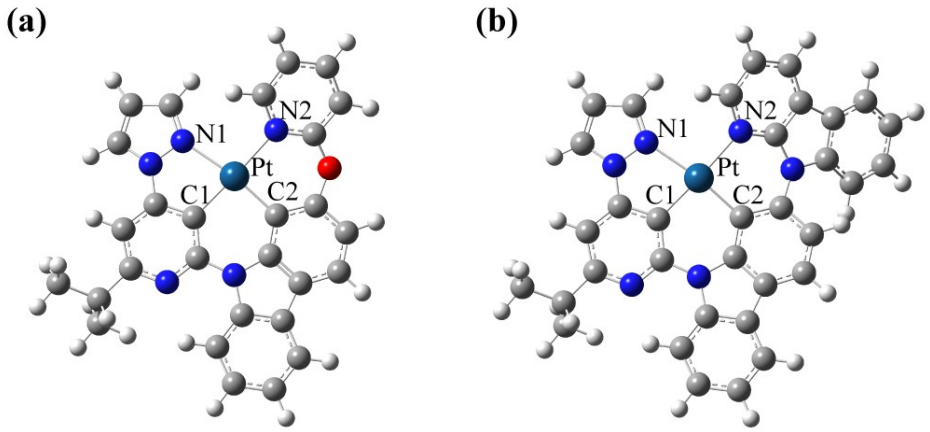

Figure S6. Molecular Skeletons.

Table S2 Selected Bond length (Å) ,Angles (deg) Dihedral Angles (deg)

	Pt(pzpy-czOpy)	Pt(pzpy-czcl)
	Bond length (Å)	
Pt-N1	2.18240	2.18288
Pt-N2	2.16051	2.15908
Pt-C1	1.97986	1.99090
Pt-C2	1.98740	1.98515
	Bond angle (deg)	
N1-Pt-N2	98.84261	97.99027
N2-Pt-C2	90.44258	90.94562
C2-Pt-C1	91.88976	92.12845
C1-Pt-N1	79.47370	79.35015
	Dihedral (deg)	
pz(cl)-py	33.66709	28.44744

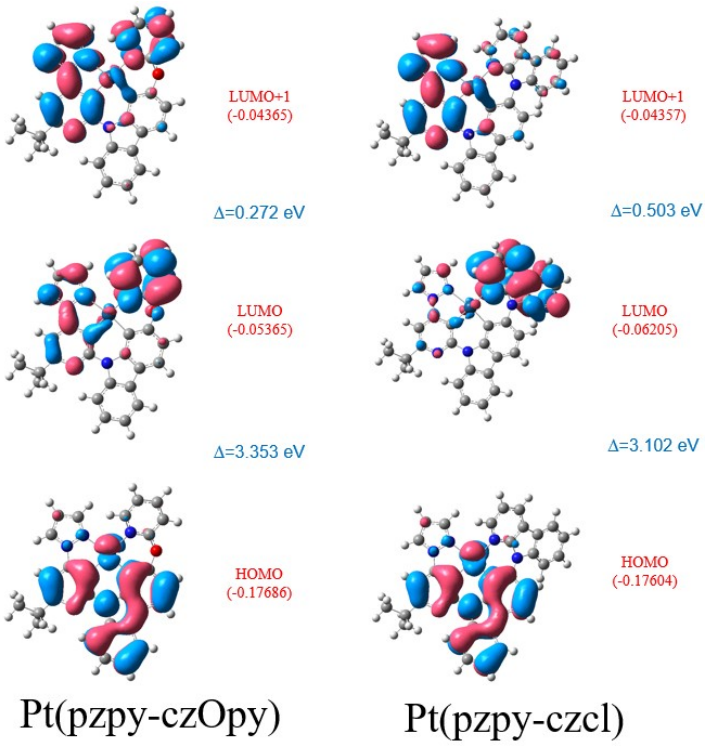

Figure S7. Frontier molecular orbitals.

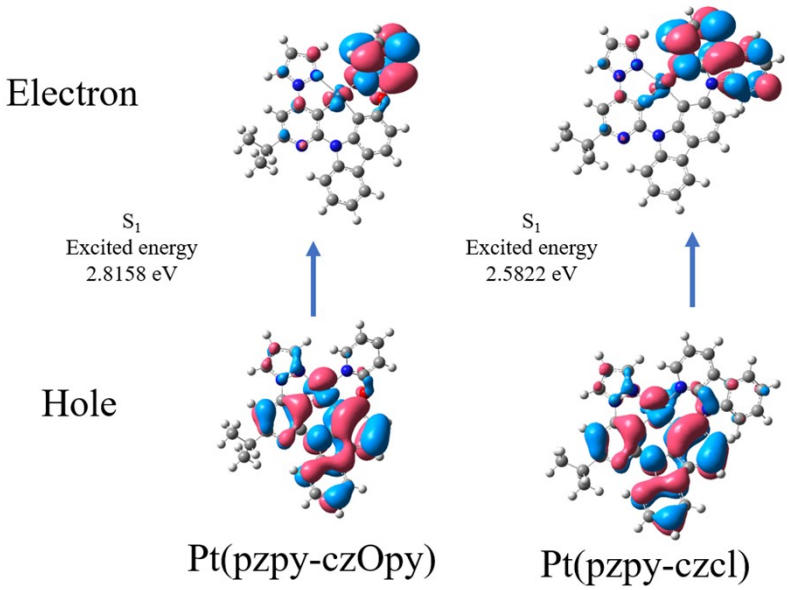

Figure S8. Electron and hole distribution on S_1

Table S3 NTOs analysis

Molecule	S_1		T_1	
	Transition orbitals	Proportions (%)	Transition orbitals	Proportions (%)
Pt(pzpy-czOpy)	HOMO→LUMO+1	3.70	HOMO→LUMO+1	27.27
	HOMO→LUMO	93.81	HOMO→LUMO	66.37
Pt(pzpy-czcl)	HOMO→LUMO	93.77	HOMO→LUMO+1	7.84
			HOMO→LUMO	80.71
	HOMO-1→LUMO	4.18		
			HOMO-1→LUMO	6.18

Table S4 Reorganization energy of molecules

Molecule	Reorganization Energy (T_1-S_0) (cm^{-1})	
	S_0	T_1
Pt(pzpy-czOpy)	1824.584	1758.104
Pt(pzpy-czcl)	2547.281	2155.658

Device performances

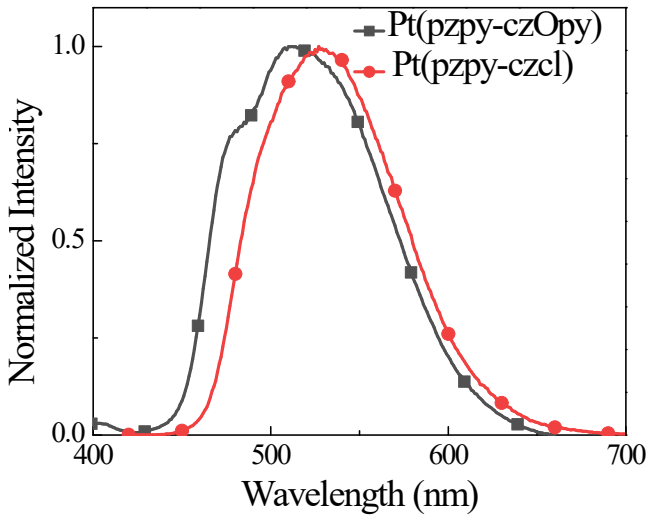

Figure S9 PL spectra of 20 wt% Pt(II) complexes in mCBP

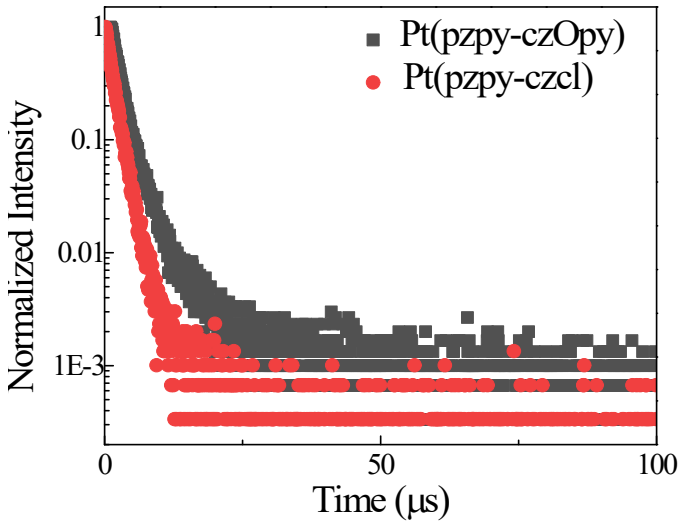

Figure S10. Transient PL decay curves of 20 wt% Pt(II) complexes in mCBP

Table S5 Photophysical data of 20 wt% Pt(II) complexes doping in mCBP

Complex	λ_{max} [nm]	FWHM [nm]	Φ [%]	ι [μs]	k_r [10^5 s^{-1}]	k_{nr} [10^5 s^{-1}]
Pt(pzpy-czOpy)	512	107	40	1.85	2.16	3.24
Pt(pzpy-czcl)	527	97	47	1.50	3.13	3.53

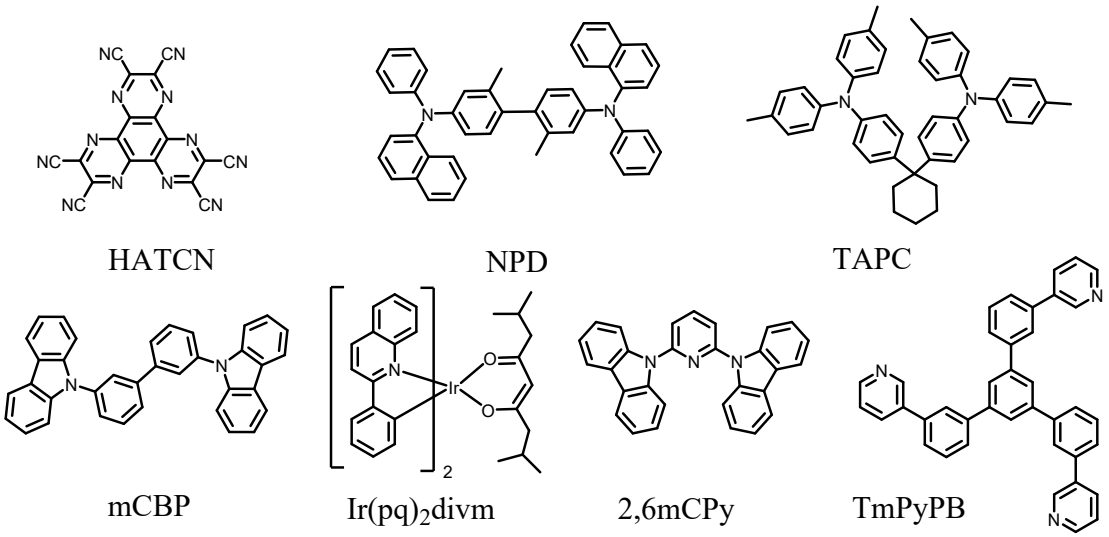

Figure S11 Structures of Functional materials used in devices.

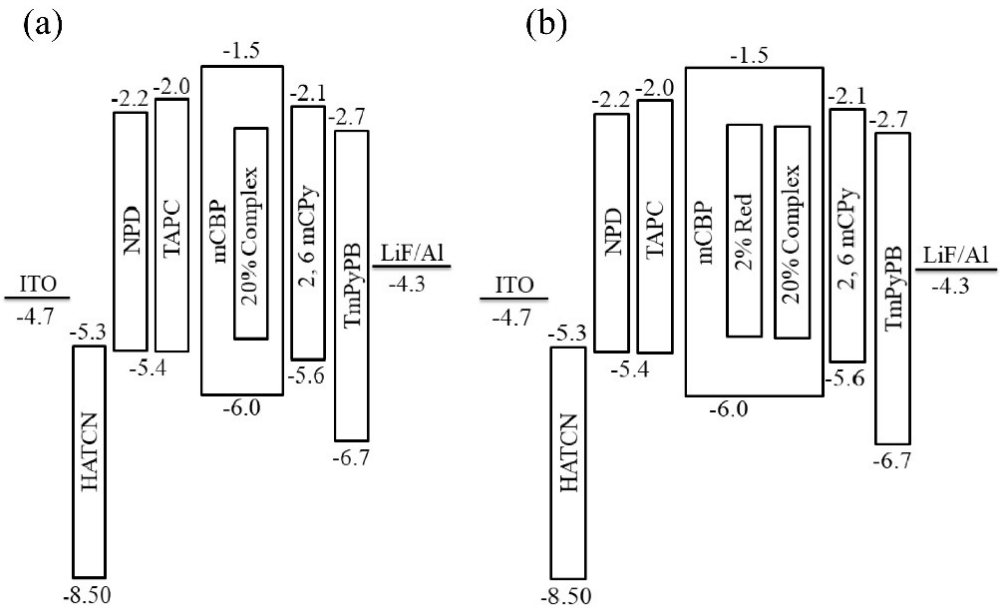

Figure S12 Device structures.

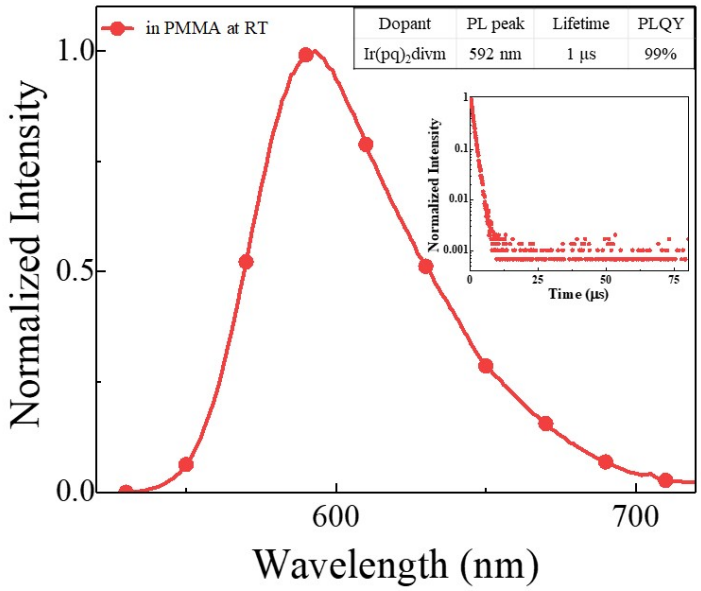

Figure S13 Photophysical properties of $Ir(pq)_2divm$

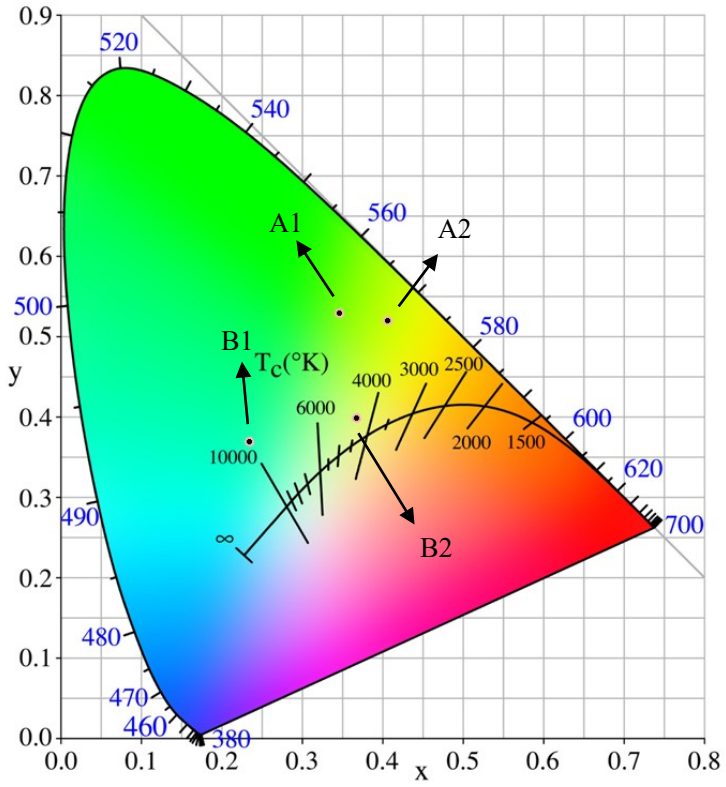

Figure S14 CIE color space chromaticity diagram of the device A and B.

^{1}H NMR and ^{13}C NMR Spectra

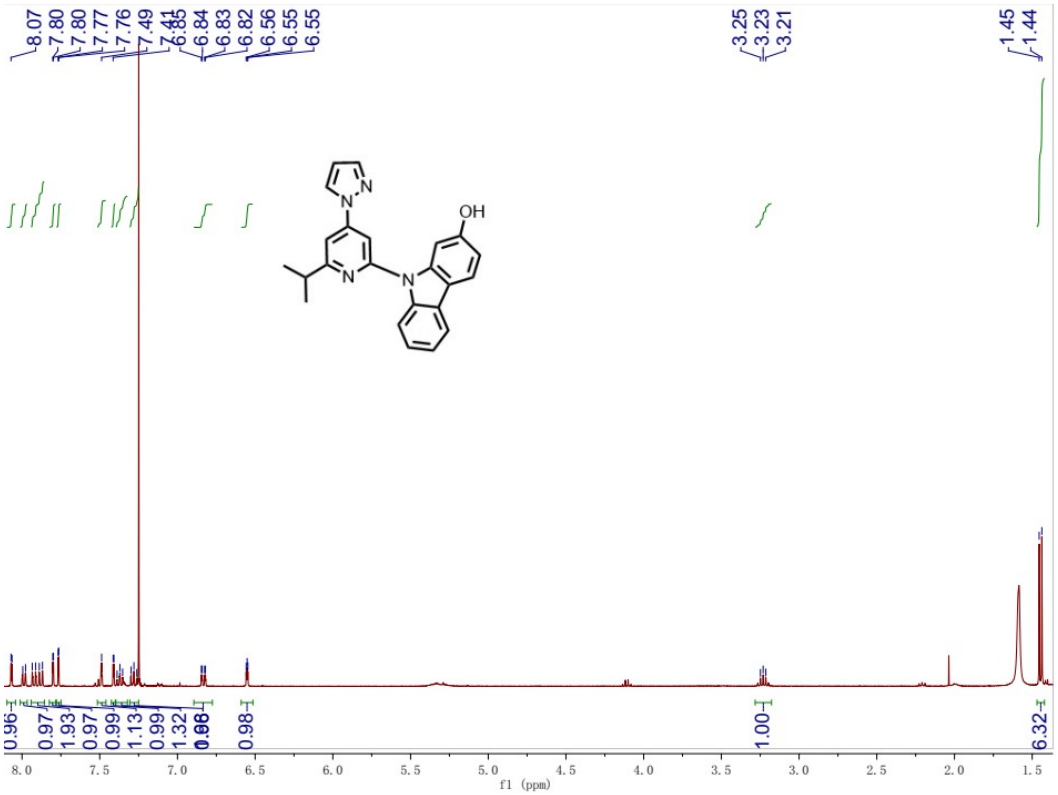

Figure S15 ^{1}H NMR of ligand **3**

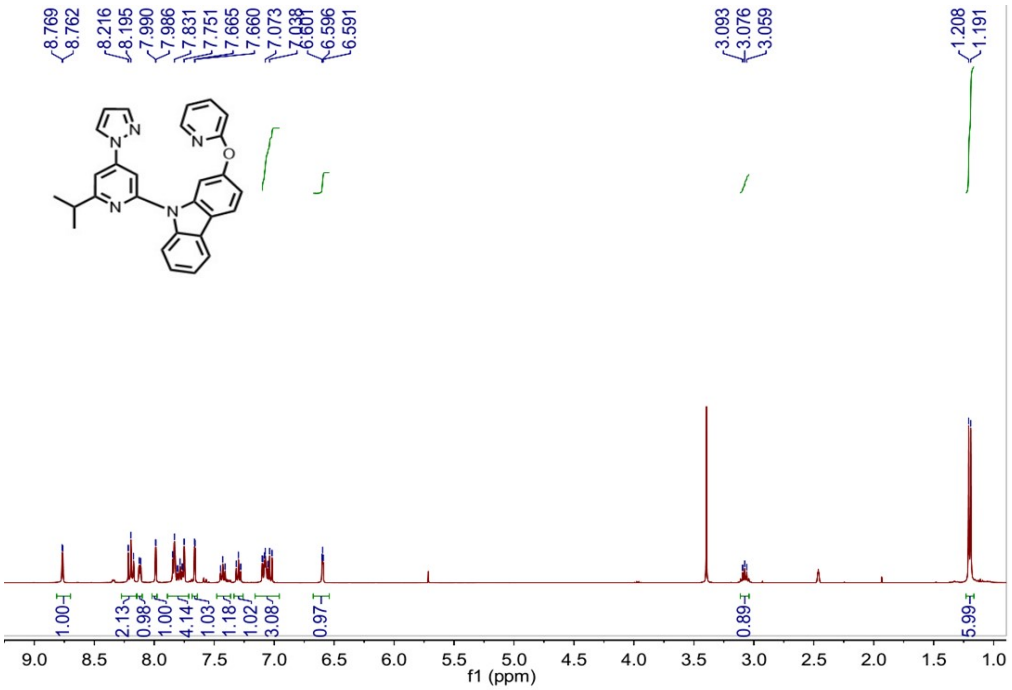

Figure S16 ^{1}H NMR of pzpy-czOpy precursor

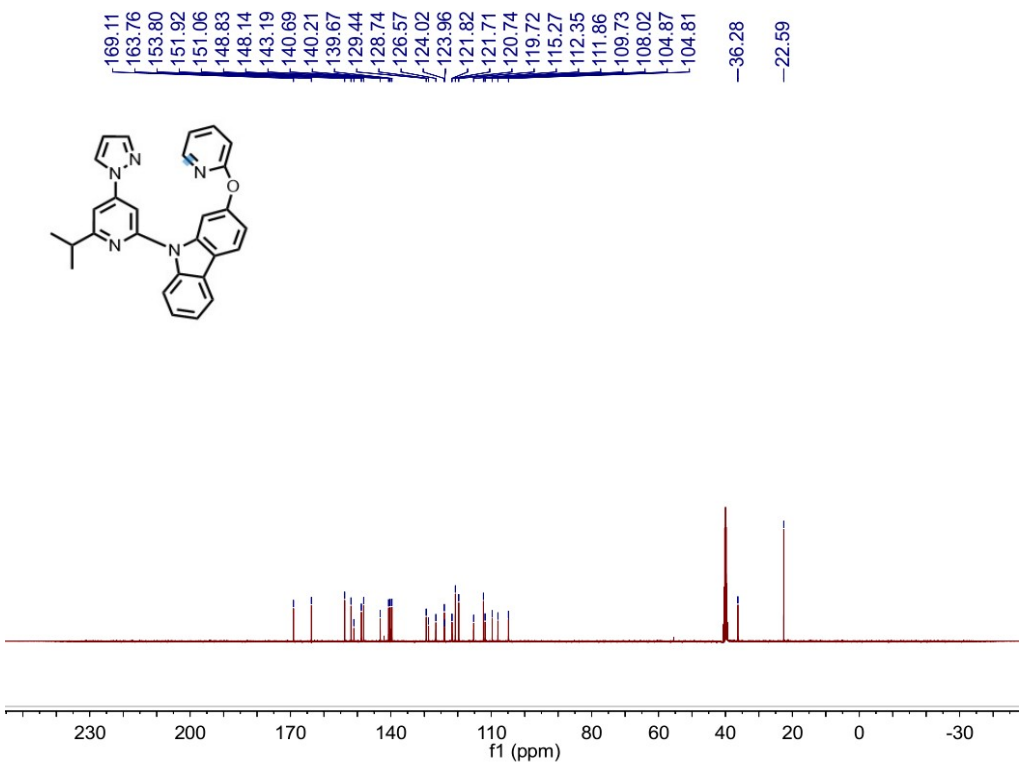

Figure S17 ^{13}C NMR of pzpy-czOpy precursor

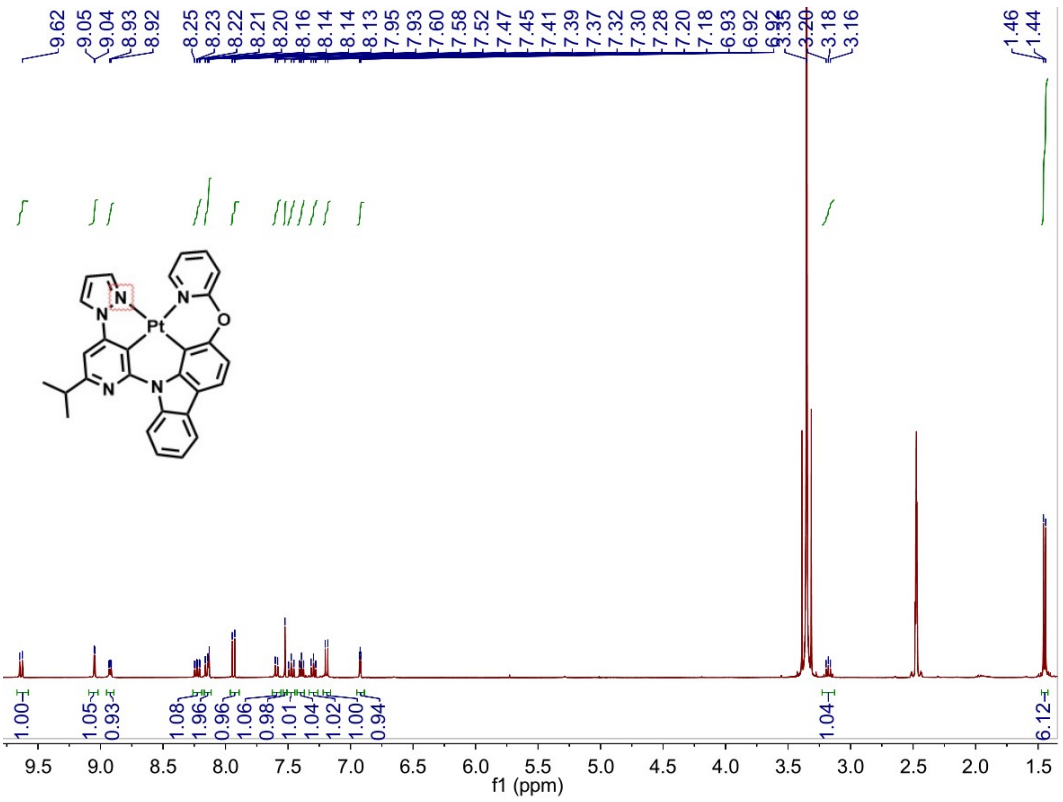

Figure S18 ^{1}H NMR of Pt(pzpy-czOpy)

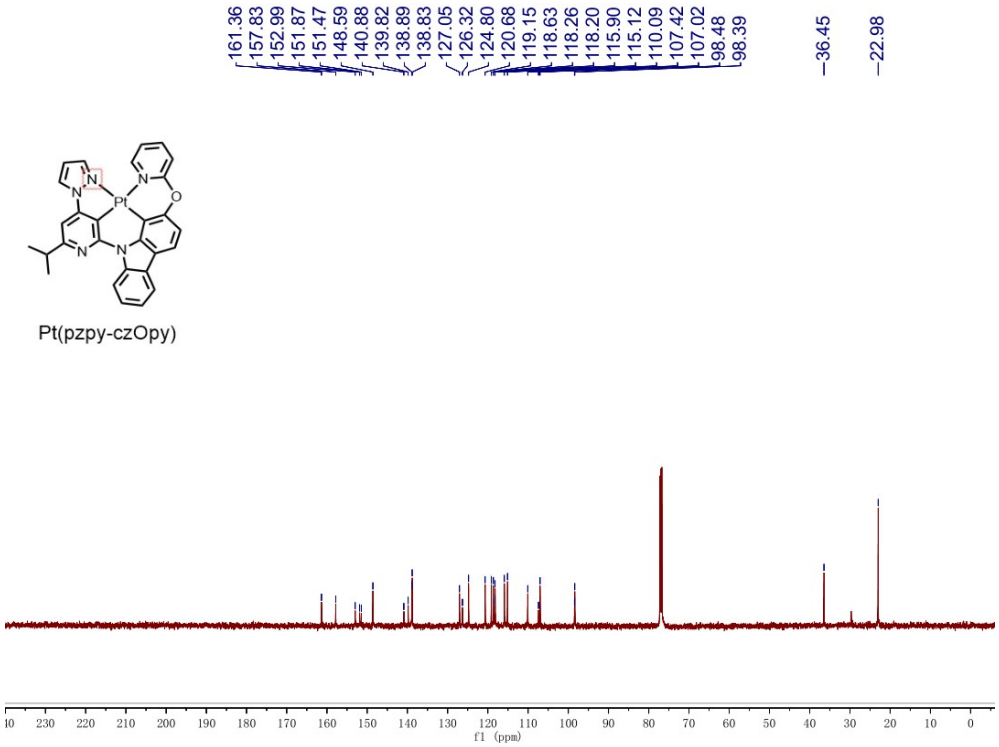

Figure S19 ^{13}C NMR of Pt(pzpy-czOpy)

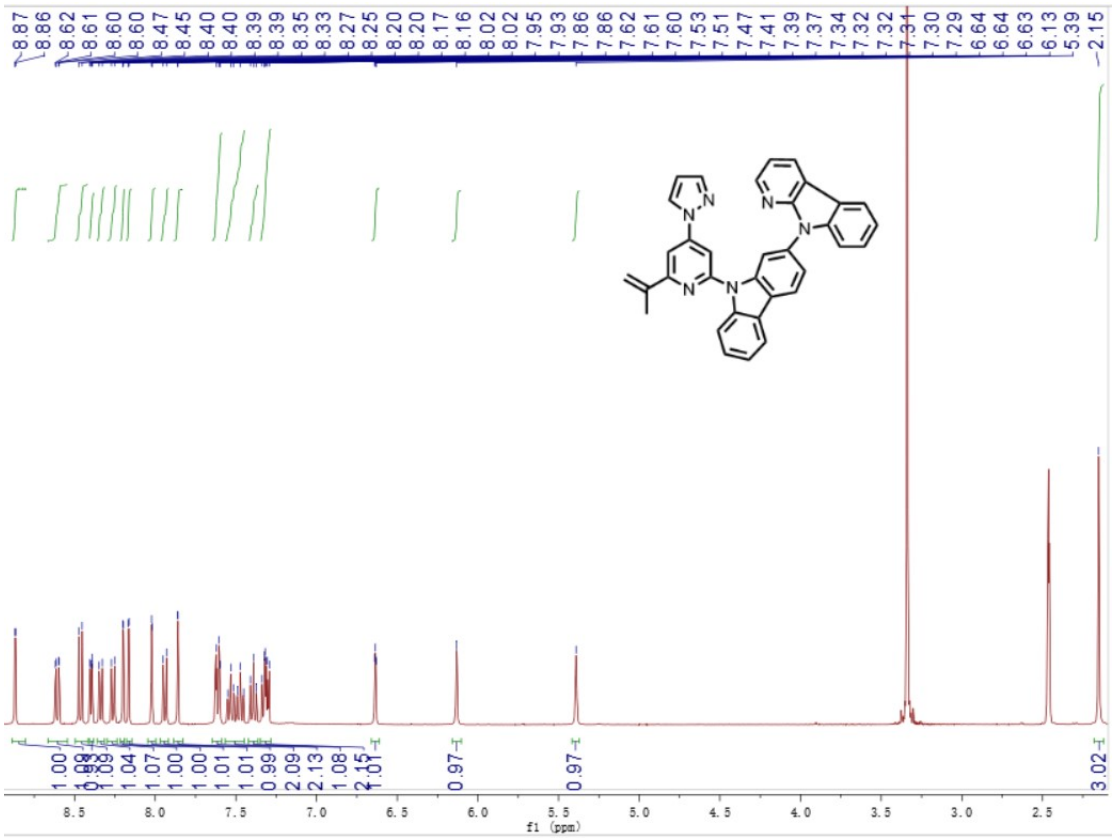

Figure S20 ^{1}H NMR of ligand **5**

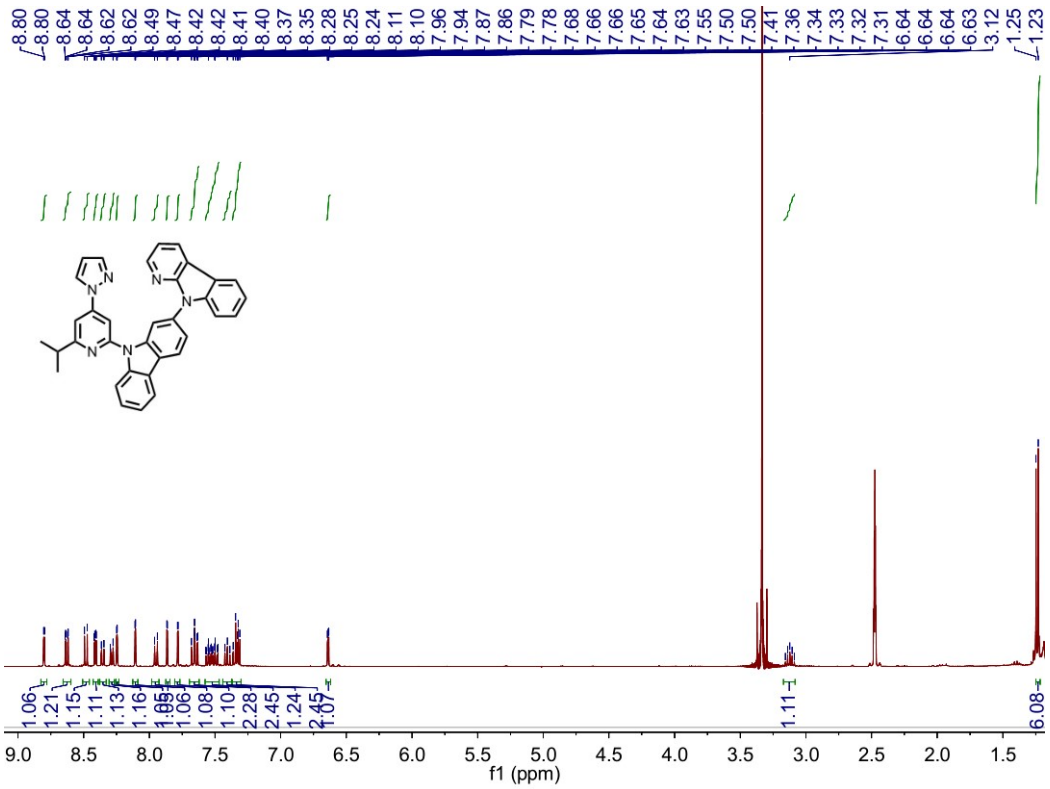

Figure S21 ^{1}H NMR of pzpy-czcl precursor

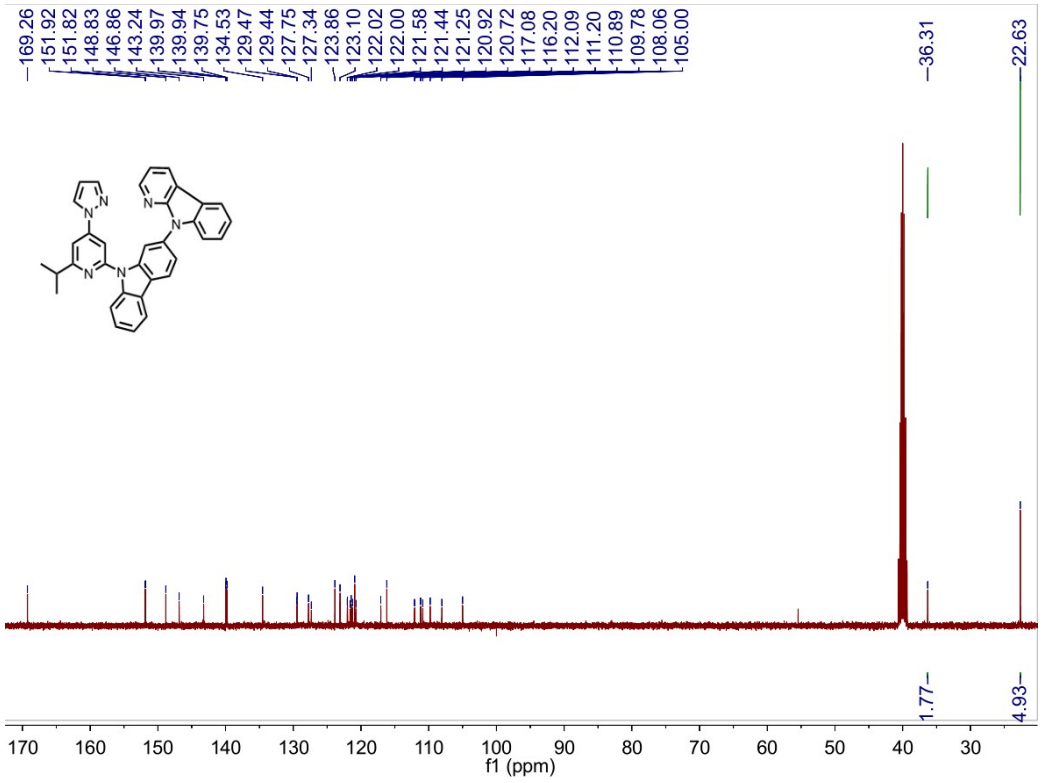

Figure S22 ^{13}C NMR of pzpy-czcl precursor

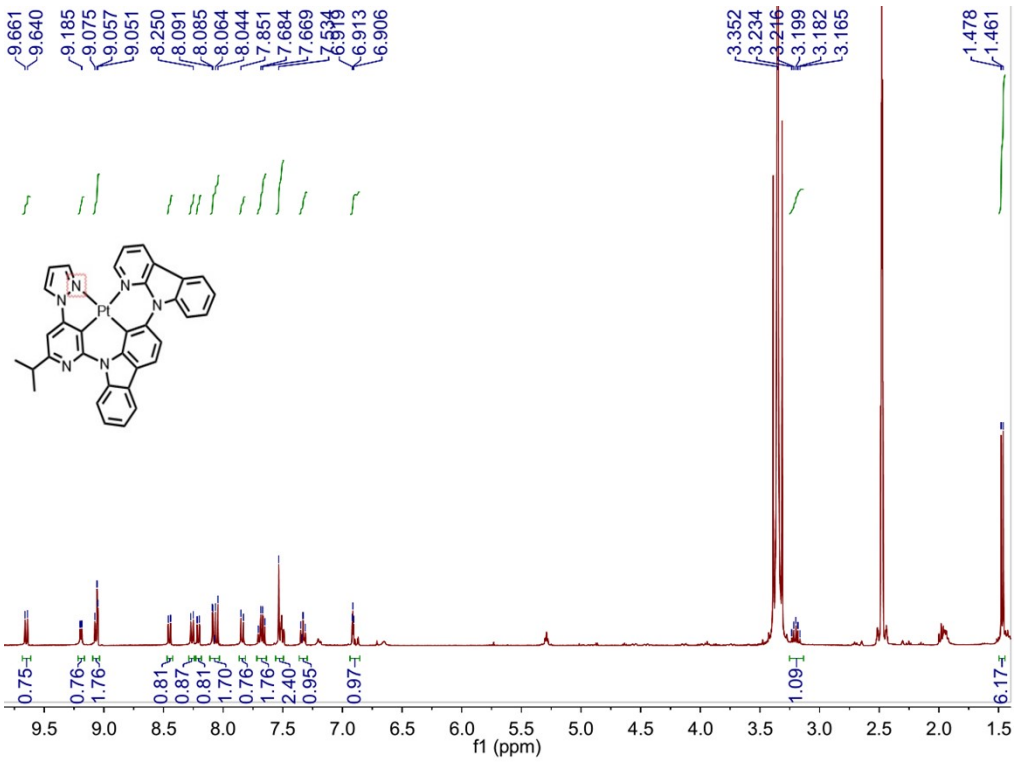

Figure S23 ^{13}H NMR of Pt(pzpy-czcl)

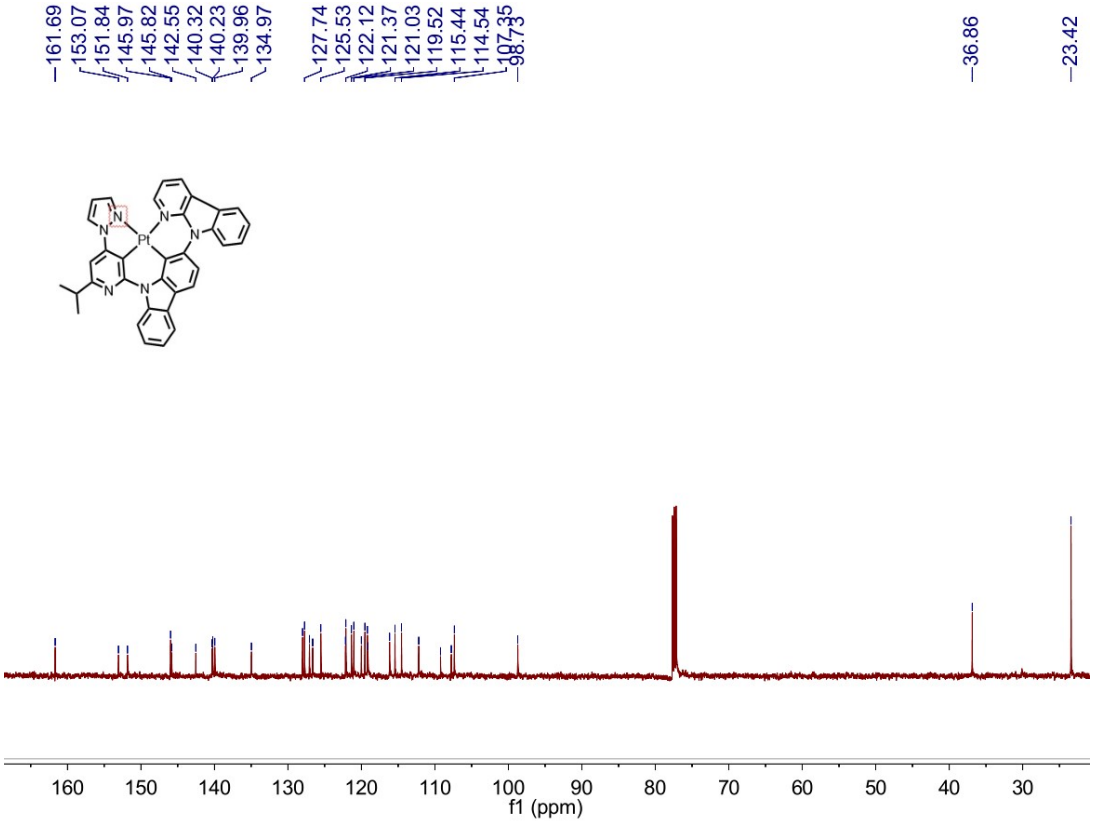

Figure S24 ^{13}C NMR of Pt(pzpy-czcl)**LC-Mass Spectra**

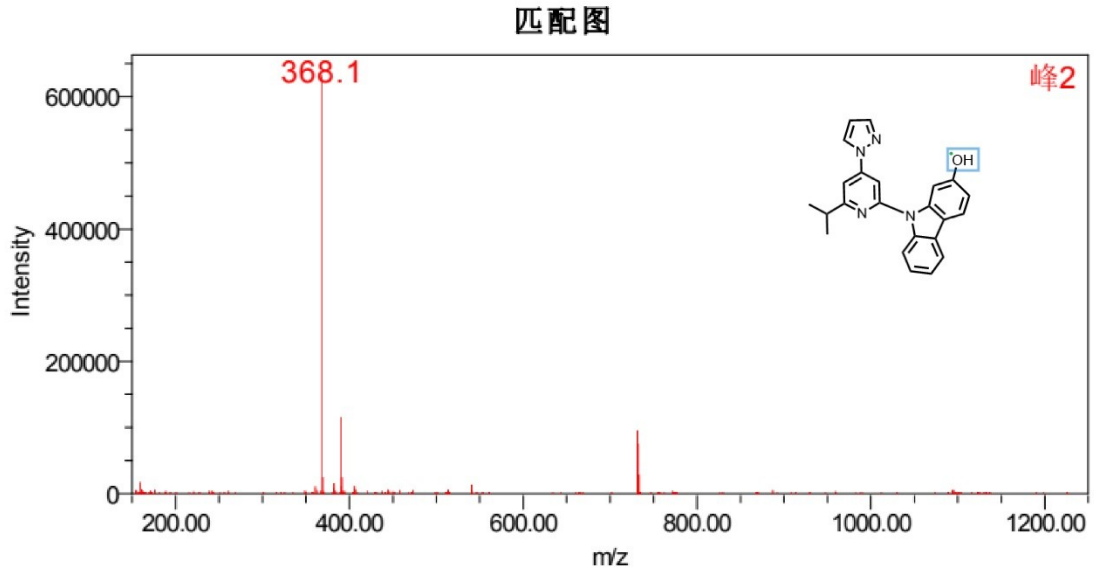

Figure S25 LC-Mass of ligand **3**

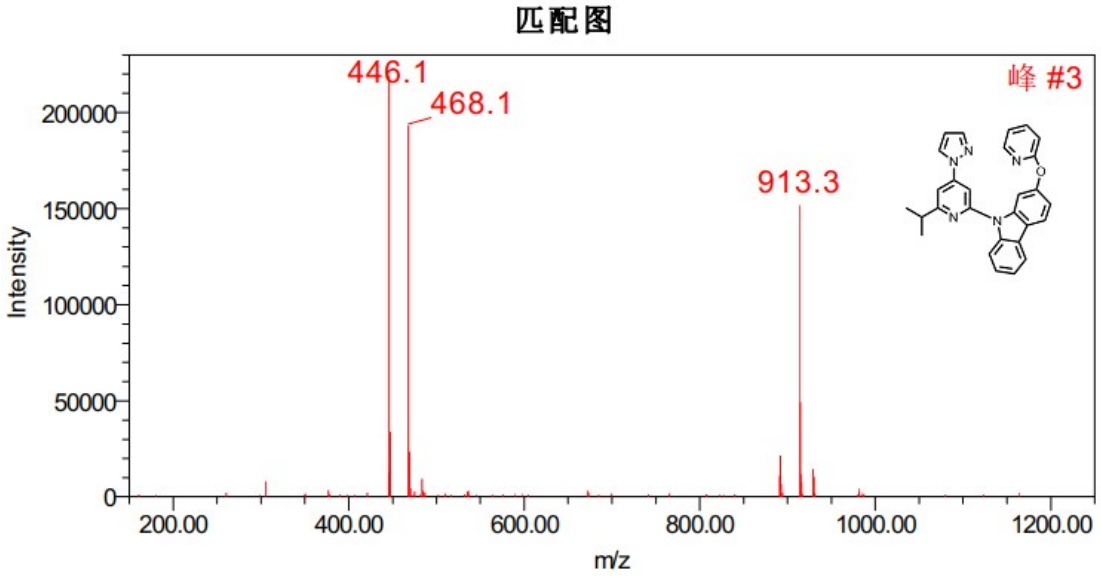

Figure S26 LC-Mass of pzpy-czOpy precursor

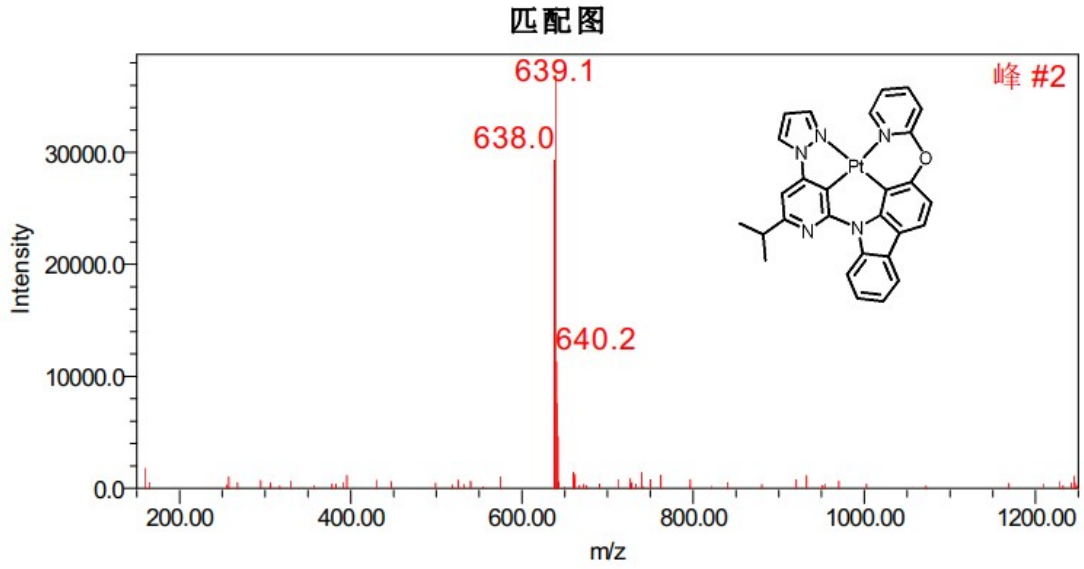

Figure S27 LC-Mass of Pt(pzpy-czOpy)

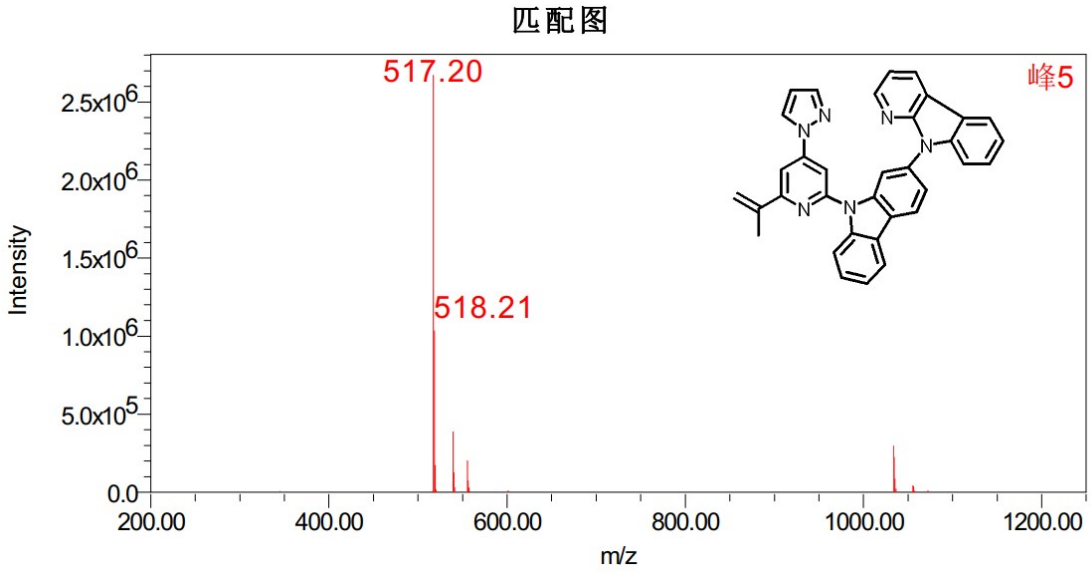

Figure S28 LC-Mass of ligand **5**

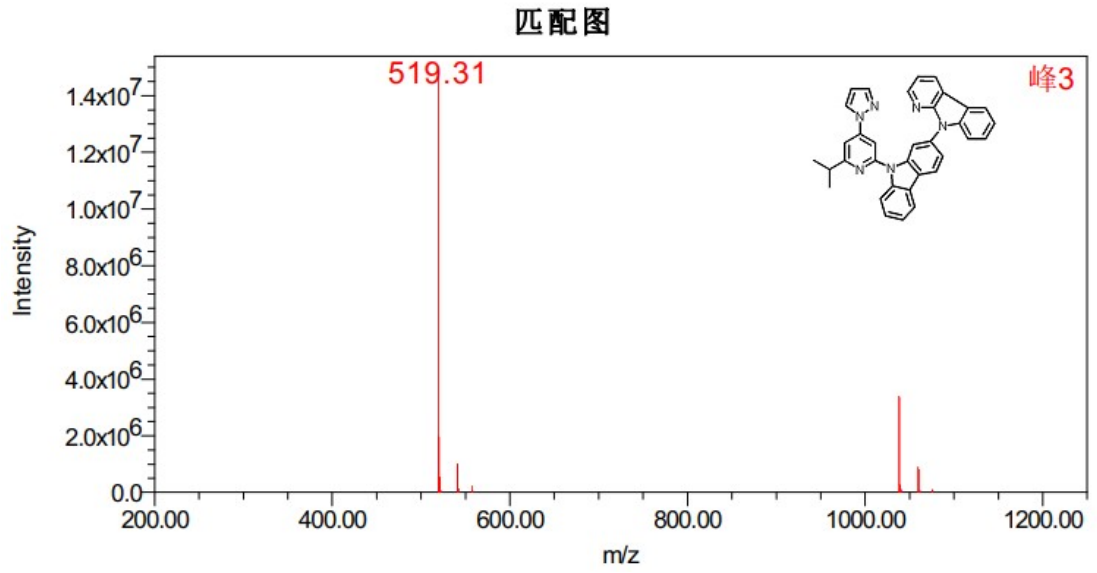

Figure S29 LC-Mass of pzpy-czcl precursor

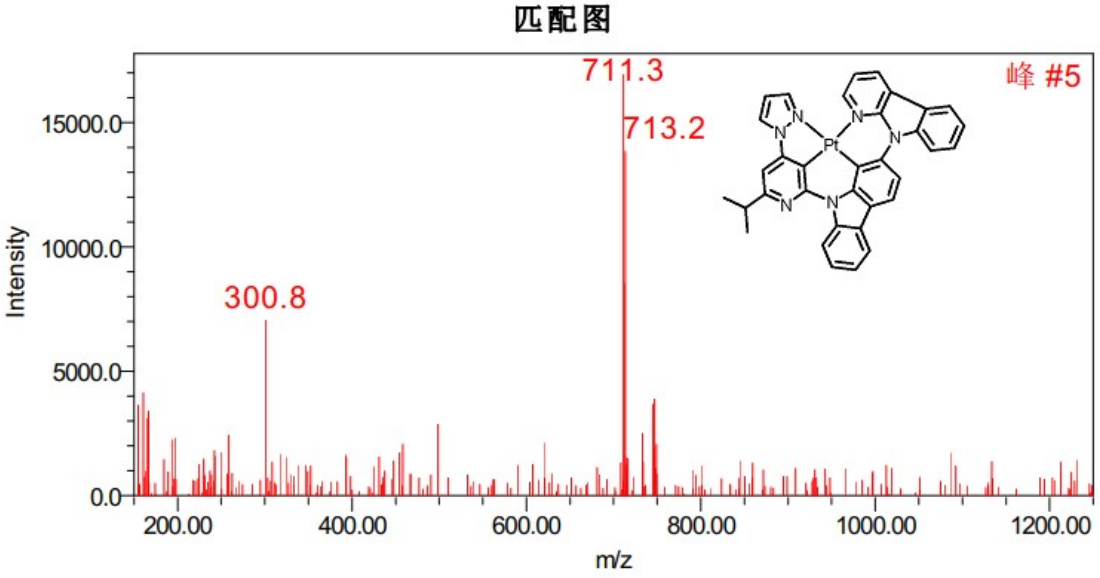

Figure S30 LC-Mass of Pt(pzpy-czcl)

HRMASS Spectra

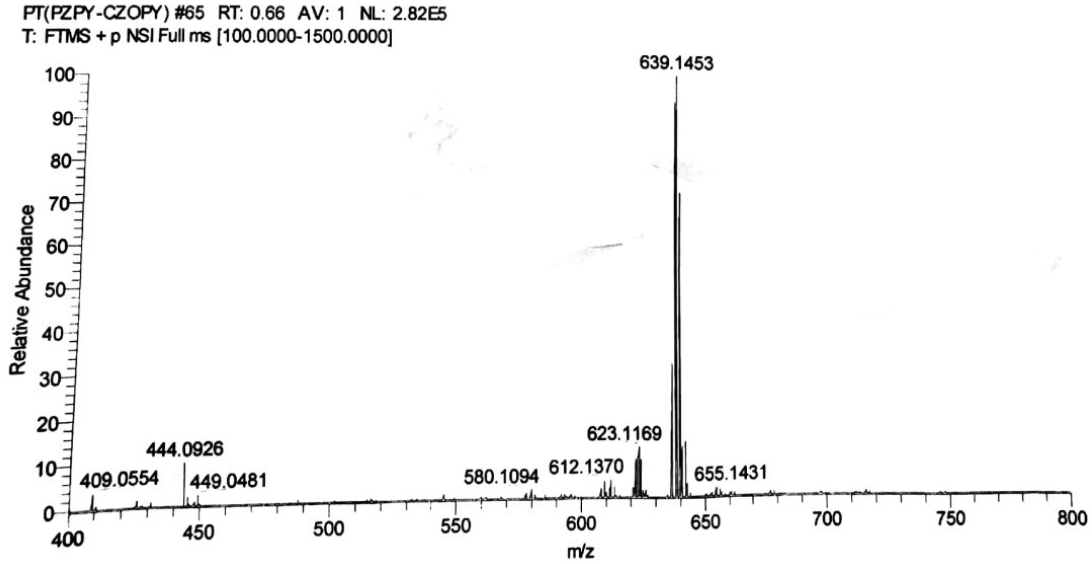

Figure S31 HRMass of Pt(pzpy-czOpy)

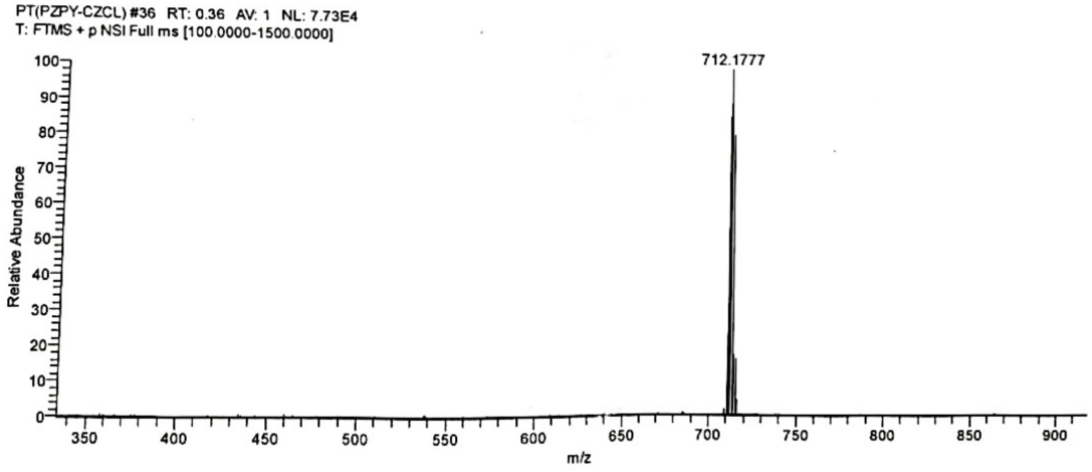

Figure S32 HRMass of Pt(pzpy-czcl)

References

[1] L. Zhu, W. Xie, C. Qian, W. Xie, K. Shen, A. Lv, H. Ma, H. Li, X. Hang, W. Li, S. Su, W. Huang, *Adv. Opt. Mater.* **2020**, *2000406*.